J Mol Model (2004) 10:38–43
DOI 10.1007/s00894-003-0167-4

ORIGINAL PAPER

Carlos H. T. P. Silva · Paulo Almeida · Carlton A. Taft

Density functional and docking studies of retinoids for cancer treatment

Received: 20 July 2003 / Accepted: 8 October 2003 / Published online: 22 November 2003

Abstract The retinoic acid receptor (RAR) and retinoid X receptor (RXR) are members of the nuclear receptor superfamily. The ligand-binding domain contains the ligand-dependent activation function. The isotypes RARα,β and γ are distinct pharmacological targets for retinoids involved in the treatment of various cancers and skin diseases. There is thus considerable interest in synthetic retinoids with isotype selectivity and reduced side effects. In this work we have focused on the retinoid acid receptor and three of its panagonists. We have carried out density functional geometry optimizations at the B3LYP/6-31G* level, computed two types of atomic charges and also electrostatic potentials. A docking program was used to investigate the interactions between the receptor and the three ligands. A theoretically more potent inhibitor, which was obtained by modifying one of the retinoic acids investigated, is proposed.

Keywords Density functional · Docking · Cancer treatment

Introduction

Ab initio and density functional theories (DFT) are proving to be very useful tools for investigating a wide range of important biological receptors and complexes. [1, 2, 3, 4, 5, 6, 7, 8, 9, 10, 11, 12, 13, 14, 15, 16, 17, 18, 19, 20] The retinoic acid receptor (RAR) and retinoic X receptor (RXR) are a large family of nuclear receptor proteins that activate transcription in the presence of retinoic acids, the biologically active metabolites of vitamin A. Both experimental and clinical work have indicated that vitamin A (retinol) and its biologically active derivatives (collectively referred to as retinoids) exert a wide variety of profound effects on vertebrate development, cellular differentiation and homeostasis. The discovery of retinoid receptors belonging to the superfamily of nuclear ligand-activated transcriptional regulators has revolutionized our molecular understanding of these receptors. Diversity in the control of gene expression by retinoid signals is generated with complexity at different levels of the signaling pathway. A major source of diversity originates from the existence of the two families, the RAR isotypes (α, β and γ) and the three RXR isotypes (α, β and γ), and their numerous isoforms. These nuclear receptors, [7] which are related to the steroid/thyroid hormone superfamily of receptors, act as ligand-dependent transcription factors for different genes. [8] Two RA configuration isomers ((*all-E*)-RA and (*9Z*)-RA) are important in their natural function. Both isomers of RA bind to RARs and activate transcription mediated by RARs homodimers or RAR/RXR heterodimers, [9, 10] but (9Z)-RA is the only known natural ligand for RXRs. [11, 13]

Analogues of retinoic acid are collectively known as retinoids, and several have shown encouraging experimental and clinical activity in cancer prevention and therapy. [14, 15] However, the clinical use of the retinoids is limited by their toxicity and teratogenicity at pharmacological doses. [16, 17] It has been suggested that both the therapeutic and toxicologic effects of RA may be mediated by RARs, RXRs and binding proteins. [18] Retinoids are involved in the regulation of cell growth, differentiation and processes that play an important role in postnatal life.

The RAR family, composed of the α, β and γ isotypes, has different pharmacological targets. The specificity of the different RAR isotypes together with the potential

C. H. T. P. Silva
Instituto de Física de São Carlos, Universidade de São Paulo,
Caixa Postal 369, São Carlos, SP, Brazil

P. Almeida
Laboratório de Biotecnologia e Ecologia de Microrganismos
do Departamento de Ciências da Biointeração
do Instituto de Ciências da Saúde, Salvador, BA, Brazil

C. A. Taft (✉)
Centro Brasileiro de Pesquisas Físicas,
Rua Dr. Xavier Sigaud 150,
CEP 22290-180 Rio de Janeiro, RJ, Brazil
e-mail: taft@cbpf.br and catff@terra.com.br

reduction of therapeutic side-effects such as teratogenicity and hypervitaminosis A syndrome, skin irritation, liver toxicity and premature growth closure lead to the necessity of finding retinoids selective for the individual RAR isotypes. The retinoid treatment of human acute leukemia refers to RARα and is a differentiation therapy. RARβ plays a central role in limiting the growth of different cell types, thereby being a possible target for the treatment of breast cancer and other cancers. On the other hand, RARγ is primarily involved in skin photo aging, carcinogenesis and in skin diseases.

Numerous synthetic agonist and antagonist retinoids differentiate RXR from RAR or are selective for the RARα, β or γ isotypes. In this work, we investigate the characteristics involved in the receptor interaction and selectivity process. The geometries of BMS184394, BMS181156 and CD564 were fully optimized at the B3LYP/6-31G* level. NBO charges [21] were calculated in the gas phase. Electrostatic effects of these agonists and panagonists were also investigated. We have performed docking studies using the DOCK 5.1.0 [19] program in order to investigate the orientation of these ligands in their respective RAR active sites as well as to measure the receptor–ligand interaction energies.

Methodology

We have used Gaussian 98 [22]at the B3YLP-6-31G*/6-31G* level for the geometry optimizations. The retinoids were fully optimized yielding stationary minimum configurations that are in agreement with the bioactive conformations. Mulliken and Natural Bond Orbital (NBO) charges [21]as well as electrostatic potentials were obtained. In principle, all docking applications include four steps, i.e. identification and preparation of the receptor site, preparation of the ligand(s), docking the ligand(s) and evaluation of the docked orientations. Docking calculations were performed using the DOCK 5.1.0 program, [19] with a grid of dimension 20×20×20 Å centered on the sulfur atom of Met272 (residue from the active site of the RAR), and a grid spacing of 0.3 Å. We have selected 33 spheres in the bioactive clusters, which were enough to fill the RAR active site. Force field (Amber) charges and hydrogen atoms were added to the protein using the Insight II program. [23] For the ligands, a flexibility algorithm (anchor-first search) and a contact_clash_overlap of 0.75 were used. The scoring function uses shape, geometry, orientation as well as force fields, whereas terms such as van der Waals and Coulombic terms are included.

Results and discussion

We give in Figs. 1, 2 and 3 the stationary forms of BMS184394-*R* (ligand of 1FCX, Fig. 1), CD564 (ligand of 1FCY, Fig. 2), BMS181156 (ligand of 1FCZ, Fig. 3) from full B3LYP/6-31G*geometry optimization in the gas phase. Our conformation is very similar to the X-ray structure of the bioactive conformation. Our calculated structures (interatomic distances, angles and dihedrals) for the 1FCX, 1FCY and 1FCZ ligands are given in Table 1. The bioactive X-ray crystal structures [20]are also given for comparison. We observe good agreement between our theoretically calculated values and the X-ray bioactive structures (interatomic distances, angles and dihedrals values).

The major difference amongst the three structures is that the 1FCY ligand contains a keto group at the 28 and 29 positions (Fig. 2), and (1FCZ ligand) contains two vinylic groups connected to C28 (Fig. 3), whereas the 1FCX ligand (Fig. 1) carries a hydroxyl moiety at the

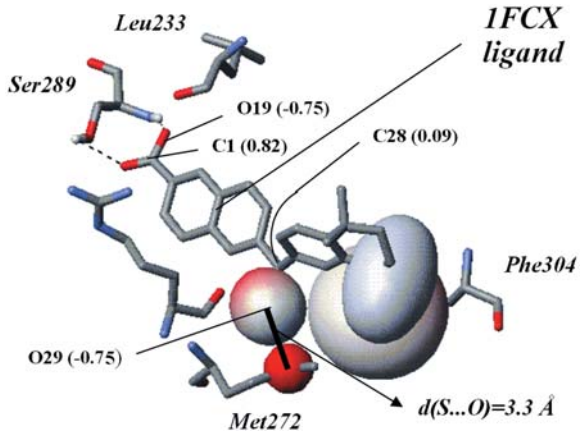

Fig. 1 BMS184394-*R* (ligand of 1FCX) and main residues of the RAR active site. NBO charges are given in parenthesis for selected atoms of the ligand. Using the van der Waals radius, the hydrophobic interaction between the phenyl ring of the Phe304 (represented as a sphere) and the closest atoms of the ligand (represented as an ellipsoid) is indicated by the contact of the two surfaces. Distances between ligand and selected residues of the active are also shown

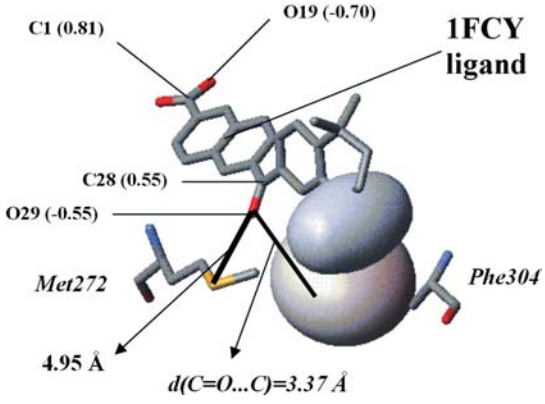

Fig. 2 CD 564 (ligand of 1FCY) and main residues of the RAR active site. NBO charges are given in parenthesis for selected atoms of the ligand. Using the van der Waals radius, the hydrophobic interaction between the phenyl ring of the Phe304 (represented as a sphere) and the closest atoms of the ligand (represented as an ellipsoid) is indicated by the contact of the two surfaces. Distances between ligand and selected residues of the active are also shown

Table 1 Interatomic distances, angles and dihedrals for retinoic acid receptor ligands

Fig. 1	1FCX X-ray	1FCX B3LYP 6-31G*	Fig. 2	1FCY X-ray	1FCY B3LYP 6-31G*	Fig. 3	1FCZ X-ray	1FCZ* 6-31G B3LYP
C28–O29	1.43	1.43	C28–O29	1.26	1.23	C10–O27	1.25	1.23
O29–H57	1.00	0.97	–	–	–	–	–	–
C21–C28	1.58	1.52	C21–C28	1.49	1.51	C10–C7	1.48	1.49
C28–C24	1.53	1.52	C28–C24	1.44	1.50	C10–C11	1.47	1.50
C1–O19	1.31	1.36	C1–O19	1.30	1.36	C1–O25	1.33	1.36
C1–O18	1.18	1.22	C1–O18	1.20	1.21	C1–O26	1.20	1.21
27–24–25–8 (χ)	0.0	0.0	25–8–13–26 (χ)	0.1	0.1	12–11–20–19 (χ)	0.1	0.2
8–25–24–28 (β)	−179.2	−179.0	26–27–24–28 (β)	−180.0	−179.0	19–20–11–10 (β)	−180.0	−179.0
11–12–13–26 (φ)	−170.0	−167.1	10–9–8–25 (φ)	−171.0	−170.0	15–14–13–12 (φ)	−165.0	−166.0
–	–	–	–	–	–	–	–	–
–	–	–	–	–	–	11–10–7–6	26.0	27.0
27–24–28–29 (γ)	−81.0	−80.2	25–24–28–29 (γ)	32.0	31.0	12–11–10–27 (γ)	25.0	25.0
22–23–6–7	−180.0	−180.1	22–23–6–7	−180.0	−179.0	–	–	–
–	–	–	–	–	–	10–7–6–5	179.3	179.0
7–2–1–18 (ε)	−160.8	−161.9	7–2–1–18 (ε)	−164.0	−163.0	3–2–1–25 (ε)	23.0	−22.7
28–21–22–23 (θ)	179.0	179.0	28–21–22–23 (θ)	179.0	178.0	7–6–5–4 (θ)	−177.6	−177.3
26–13–12–16 (ϕ)	−53.2	−52.0	16–12–13–26 (ϕ)	−51.0	−50.0	12–13–14–22 (ϕ)	−45.6	−45.9
14–9–8–25 (α)	65.8	64.9	25–8–9–14 (α)	69.0	68.0	19–18–17–24 (α)	71.7	71.5

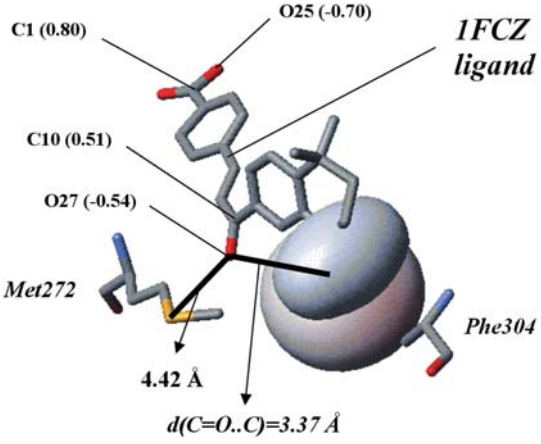

Fig. 3 BMS181156 (ligand of 1FCZ) and main residues of the RAR active site. NBO charges are given in parenthesis for selected atoms of the ligand. Using the van der Waals radius, the hydrophobic interaction between the phenyl ring of the Phe304 (represented as a sphere) and the closest atoms of the ligand (represented as an ellipsoid) is indicated by the contact of the two surfaces. Distances between ligand and selected residues of the active are also shown

same position. The different structures result in a 1FCX ligand, which is γ-selective, 1FCY ligand, which is both β- and γ-selective, and 1FCZ ligand, which is α-, β- and γ-selective (panagonist). The predominant contributions of the 1FCX ligand to the RARγ-selectivity can be attributed to the interaction of the Met272 residue from the receptor with the close (3.29 Å) hydroxyl group (Fig. 1). For the 1FCY ligand both the Met272 and Phe304 residues from the receptor are closest to the ligand, whereas the distance between the oxygen of the keto group and the sulfur of the Met272 has increased from 3.29 Å in 1FCX and to 4.95 Å in 1FCY. In compensation, we now observe a distance of 3.37 Å between the keto oxygen and the closest carbon of the Phe304, which suggests a favorable geometry for hydrogen bonding. In the case of the 1FCZ complex, the sulfur atom of Met272 is oriented away from the ligand (4.95 Å) and the shortest distance to Met272 corresponds to van der Waals contacts (3.64 Å) between the keto group and the closest carbon of Met272. In all three ligands, γ-selectivity is achieved through a hydrogen bond with Met272. 1FCZ has contacts with the carbons of Phe304 (3.347) and Met (3.21 Å), suggesting the presence of C–H...O=C hydrogen bonds that certainly contribute to the high activity of this panagonist. We note that, in addition to the distance between Met272 and the ligand, we must also have an appropriate charge distribution determined by the atoms connected to C28 (Figs. 1, 2 and 3) in order to promote stronger hydrogen bonding. Changing the nature of the linker from ketone to alcohol causes a loss of binding to all three isotypes, but some binding affinity is regained by the formation of the hydrogen bond. These conclusions stimulated us to investigate other linkers via docking procedures in order to search for more potent retinoids.

Our calculations of the Mulliken and NBO charges for 1FCX, 1FCY and 1FCZ in the gas phase at the B3LYP/6-31G* level yields similar trends. We give in Figs. 1, 2 and 3 the relevant carbon and oxygen NBO charges. The O29 charge (–0.750 a.u.) of the FCX ligand is larger than the charge of O29 (–0.546 a.u.) from the 1FCY ligand and the corresponding O27 atomic charge (–0.536 a.u.) of the 1FCZ ligand. The 1FCX inhibitor is an alcohol with the appropriate orientation of the hydroxyl moiety attached at the chiral center (C28) and its hydroxyl hydrogen H57 has a large positive charge (0.483 a.u.), which can facilitate interaction with a nearby polar residue from the receptor. One of the most important bioactive interactions occurs between the hydroxyl moiety (O29 atom and its hydrogen H57) and the Met272 residue of the receptor. The sulfur

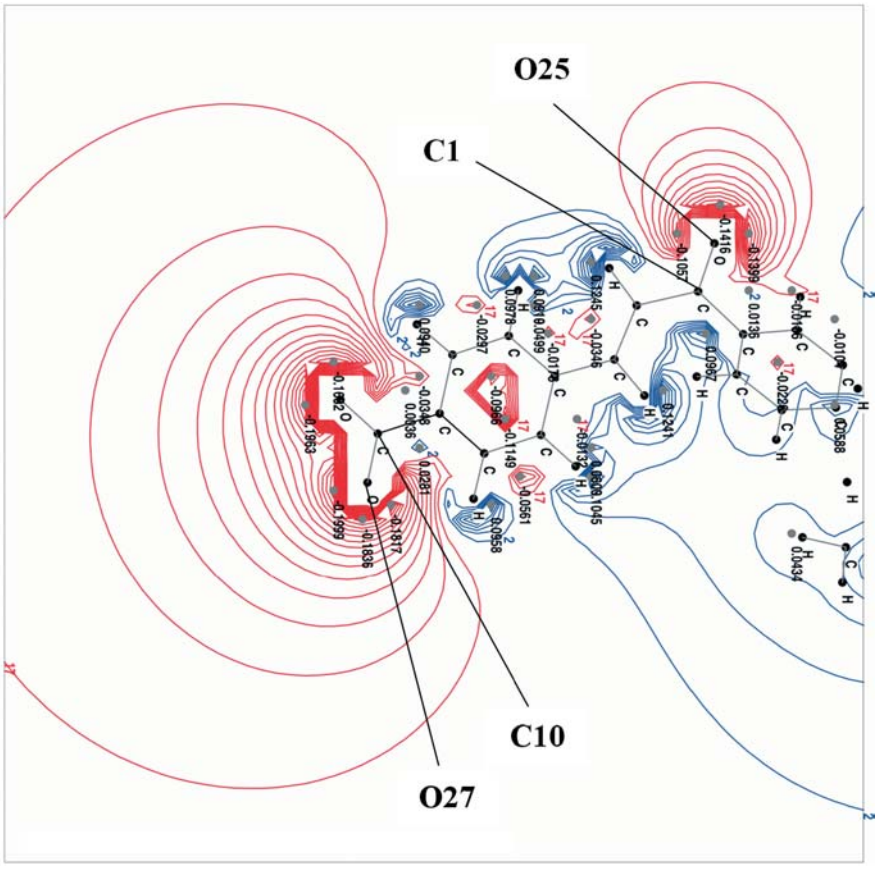

Fig. 4 Electrostatic potential of 1FCZ ligand

atom of the receptor Met272 is separated by a distance of 3.29 Å from the oxygen atom of the ligand hydroxyl moiety (Fig. 1), which suggests a hydrogen bond that is within the range of typical distances between hydroxyl and thioether groups. There also seems to be some hydrophobic interaction between Phe304 and the two methyl groups located at the opposite terminals of the carboxylate.

1FCY and 1FCZ ligands (Figs. 2 and 3, respectively) are ketones, and thus there is an increase of electrons on the O29 atom (of the hydroxyl moiety) from the1FCX ligand when its alcohol group is compared to the keto group in the 1FCY and 1FCZ ligands. The charge (0.091 a.u.) of the C28 atom, to which the hydroxyl moiety is connected, is smaller in magnitude than the corresponding keto C28 charges of 0.553 a.u. and 0.514 a.u. for the 1FCY and 1FCZ ligands, respectively.

We have calculated the electrostatic potentials for the three ligands. In Fig. 4, we give the electrostatic potential for the panagonist 1FCZ ligand. We clearly observe the possibility of two strong interaction sites due the oxygen atoms O27 (–0.536 a.u.) and O29 (–0.699 a.u.), indicated by strong negative electrostatic potentials which may participate in electrostatic and/or hydrogen bonds. Our calculated electrostatic potentials indicate, as expected, that one position is due to the presence of the hydroxyl moiety in the 1FCX ligand and the keto substituent group in the both 1FCY and 1FCZ ligands. The other one is due to the presence, in all the ligands, of the carboxylate group connected to the phenyl (or naphtyl in 1FCY and 1FCZ ligands) terminal of the molecules.

The 1FCX ligand has a lower ionization potential (I.P.=5.92 eV) and electron affinity (E.A.=1.45 eV) than the other two ligands (1FCY ligands, with I.P.=6.42 eV and E.A.=2.26 eV; 1FCZ ligand, with I.P.=6.60 eV and E.A.=2.42 eV). In particular, if we consider the simple frontier orbital approximation we note that the energy gap between the HOMO of 1FCX ligand and the LUMO of Met272 is smaller (5.12 eV) than the corresponding gaps of the other two ligands (1FCY, with gap=5.61 eV and 1FCZ, with gap=5.80 eV). Within the limitations of this approximation, these results also support a preferred interaction between the 1FCX ligand and Met272.

In order to propose new and more potent retinoic acid receptor inhibitors, we have used the DOCK 5.1.0 [19] program, and the crystal structures of the ligands with our theoretical charges. For docking calculations, we added and orientated hydrogens in the receptor, excluding the ligands. In order to determine the best orientations of the inhibitors inside the active site of the retinoic acid receptor, a docking single was performed for all the three ligands and the results obtained are in excellent agreement with the X-ray of the bioactive orientations for 1FCX inhibitor (Fig. 5a), 1FCY inhibitor (Fig. 5b) and 1FCX inhibitor (Fig. 5c). DOCK also was successful in the given scores (energy score for 1FCX inhibi-

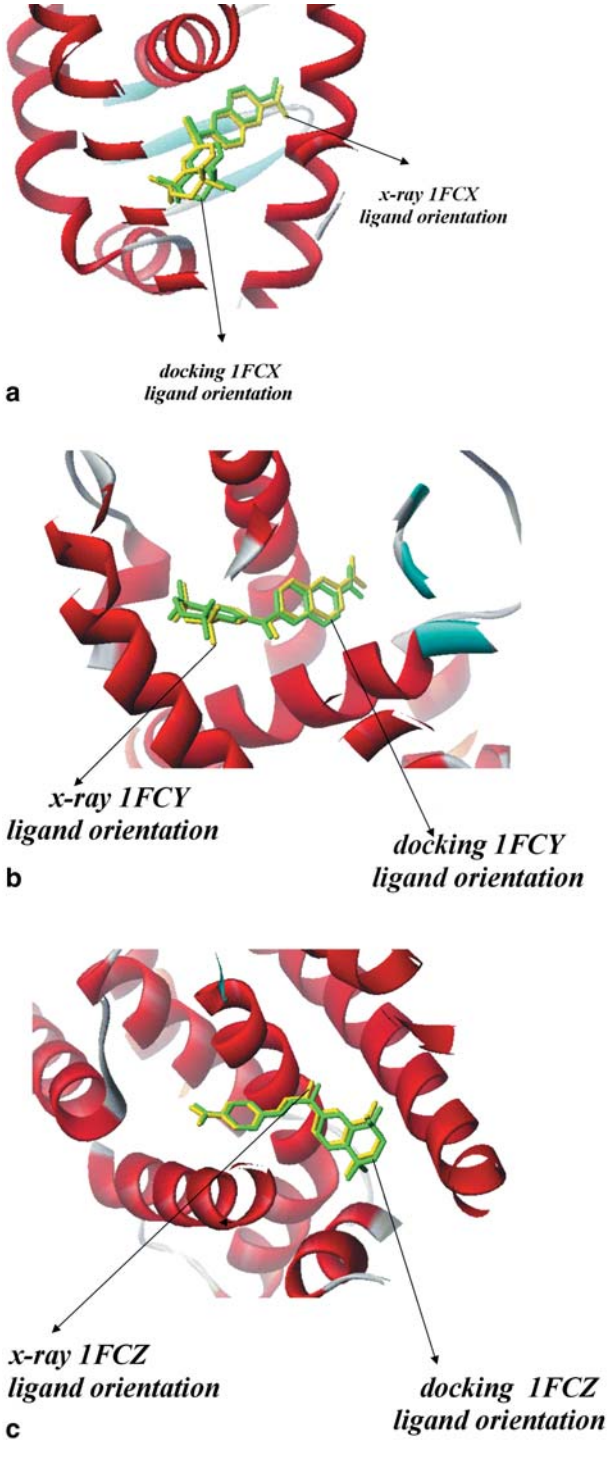

Fig 5 **a** Dock result for the 1FCX–ligand complex. Crystal structure of the ligand, superposed with the highest score orientation (in *green*) obtained with the DOCK 5.1.0 program. **b** Dock result for the 1FCY–ligand complex. Crystal structure of the ligand, superposed with the highest score orientation obtained with the DOCK 5.1.0 program. **c** Dock result for the 1FCZ-ligand complex. Crystal structure of the ligand, superposed with the highest score orientation obtained with the DOCK 5.1.0 program

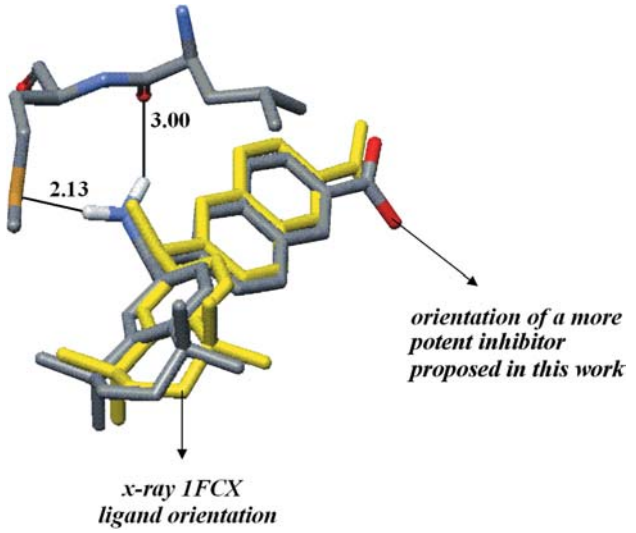

Fig. 6 Superposition of the crystal structure (Å) of the 1FCX ligand with the proposed new inhibitor

tor=−32.04 kcal mol^{-1}; energy score for 1FCY inhibitor=−28.71 kcal mol^{-1}; energy score for 1FCZ inhibitor=−27.50 kcal mol^{-1}), suggesting the 1FCX inhibitor as the most potent.

We then decided to use the DOCK 5.1.0 program to propose an even more potent retinoic acid receptor inhibitor. By inspection, the most interesting choices seem to be the replacements of the carbon 28 by a nitrogen atom, and the replacement of the oxygen 29 by an amino group. These calculations gave for the second replacement (carbon 29 by an amino group) the highest energy score of −35.0 kcal mol^{-1}. Our new proposed, theoretically more potent inhibitor is shown in Fig. 6. We also show for comparison the bioactive orientation of the 1FCX inhibitor.

Conclusions

The human retinoic acid receptor isotypes RARα,β and γ are distinct pharmacological targets for retinoids involved in the treatment of various skin diseases and cancers. Numerous retinoids have been synthesized that are aimed to be more isotype specific and less extensive in their side-effects. In this work, we have investigated, using various theoretical models, the panagonist BMS181156 (1FCZ ligand), RARβ/γ CD564 (1FCY ligand) and RARγ-selective retinoid BMS184394 (1FCX ligand). These structures provide good examples of synthetic ligands that exhibit either partial or no isotype selectivity. We note that the hydroxyl group of RARγ-selective ligands is a prerequisite for RARγ selectivity due to the hydrogen bond formed with the sulfur atom of Met272. The question of RARβ/γ versus RARγ selectivity can be attributed to this specific hydrogen bond, since its absence leads either to RARβ/γ-selective agonists like CD564 or to panagonists as BMS181156. The DOCK 5.1.0 program

indicates, however, that the replacement of the hydroxyl group by an amino group may also lead to an isotype selectivity. Full geometry optimization of the ligands and analysis of Mulliken and NBO charges (which have showed similar trends), electrostatic potentials, solvent effects, frontier orbitals, energy gaps, were also used to improve our comprehension of the behavior of these important synthetic retinoids.

Acknowledgements We acknowledge financial support from FAPERJ, FAPESP, PRONEX, CNPQ (Brasil). We thank Marcelo E. Banja for his participation.

References

1. (a) Arissawa M, Taft CA, Felcman J (2003) Int J Quantum Chem 93:422–432; (b) Martins JBL, Perez MA, Silva CHTP, Taft CA, Arissawa M, Longo E, Mello PC, Stamato FMLG, Tostes JGR (2002) Int J Quantum Chem 90:575–586
2. Martins JBL, Taft CA, Perez MA, Stamato FMLG, Longo E (1998) Int J Quantum Chem 69:117-128
3. Pavão AC, Taft CA, Guimarães TCF, Leão MBC, Mohallem J, Lester WA (2001) J Phys Chem A 105:5–11
4. Blaney FE (1999) Int J Quantum Chem 73:97–111
5. Ponder MS, Long A, Williams LM, Hamilton TP and Muccio DD (2001) J Mol Struct (THEOCHEM) 549:39–45
6. Rosen J, Day A, Jones TK, Jones TT, Nadzan AM, Stein RB (1995) J Med Chem 38:4855-4874
7. Gudas L (1994) J Biol Chem 269:15399–15402
8. Petkovich M, Brand NJ, Krust A, Chambon P (1987) Nature 330:444–450
9. Allenby G, Janocha R, Kazmer S, Speck J, Grippo JF, Levin AA (1994) J Biol Chem 269:16689–16695
10. Mangelsdorf DJ, Ong ES, Dyck JA, Evans RM (1990) Nature 345:224–229
11. Levin AA, Sturzenbecker LJ, Kazmer S, Bosakoki T, Juselton C, Allenby G, Speck J, Kratzeisen C, Rosenberger M, Lovey A, Grippo JF (1992) Nature 355:359–361
12. Zhang XK, Lehmann JM, Hoffmann B, Dawson MI, Cameron J, Graupner G, Hermann T (1992) Nature 358:587–591
13. Moon RC, Mehta RG, Rao KVN (1994) In: Spoon MB, Roberts AB, Goodman DS (eds) The retinoids biology, chemistry and medicine, 2nd edn. Raven Press, New York, pp 573–630
14. Nazdan AM (1995) Reports in medicinal chemistry, vol 30. Academic Press, New York, pp 119–128
15. Hixson EJ, Denine EP (1978) Toxicol Appl Pharmacol 44:29–40
16. Adams J (1993) Neurotoxicol Teratol 15:193–202
17. Muccio DD, Brouillete WJ, Alam M., Vaezi MF, Sani BP, Venepally P, Reddy L, Li E, Norris AW, Simpson-Herre L, Hill DL (1996) J Med Chem 39:3625–3635
18. Klaholz BP, Mitschler A, Belema M, Zus C, Moras D (2000) Proc Natl Acad Sci USA 97:6322–6327
19. Ewing TJ, Makino S, Sillman AG, Kuntz ID (2001) J Comput-Aided Mol Des 15:411–428
20. Klaholz BP, Mitschler A, Moras D (2000) J Mol Biol 302:155–170
21. Foresman JB, Keith TA, Wiberg KB, Snoonian J, Frisch MJ (1996) J Phys Chem 100:16098-16104
22. Frish MJ, Trucks GW, Schlegel HB, Scuseria GE, Robb MA, Cheeseman JR, Zarkzewski VG, Montgomery JA, Stratmann RE, Burant JC, Dapprich, S, Millam JM, Daniels AD, Kudin KN, Strain MC, Farkas O, Tomasi J, Baone V, Cossi M, Cammi R, Mennucci B, Pomelli C, Adamo C, Clifford S, Ochterski J, Peterson GA, Ayala PY, Cui Q, Morokuma K, Makick DK, Rabuck AD, Raghavachari K, Foresman JB, Cioslowski J, Ortiz JV, Stefanox BB, Liu G, Kiashenko A, Piskorz P, Komaromi I, Gomperts R, Martin RL, Fox DJ, Keith T, Al-laham MA, Peng CY, Nanayakkara A, Gonzales C, Challacombe M, Gill PMW, Johnson BG, Chen W, Wong MW, Andres JL, Head-Gordon M, Repogle ES, Pople JA (2002) Gaussian 98 (revision A11), Gaussian, Pittsburgh, Pa.
23. Insight II User guide, version 2000 (2000) Accelrys, San Diego, Calif.